Title
Comparison of Wavelet Image Coders Using the Picture Quality Scale (PQS)

Authors
Lu, Jian
Algazi, Ralph
Estes, Robert R.

Publication Date
1995

Peer reviewed

Comparison of Wavelet Image Coders Using the Picture Quality Scale (PQS)

Jian Lu, V. Ralph Algazi, and Robert R. Estes

Center for Image Processing and Integrated Computing (CIPIC)
University of California, Davis, CA 95616
Tel: (916)752-2387 Fax: (916)752-8894
E-mail: {jian,algazi,estes}@cipic.ucdavis.edu

ABSTRACT

Image coding is one of the most visible applications of wavelets. There has been increasing number of reports each year since the late 1980's on the design of new wavelet coders and variations to existing ones. In this paper, we report some results from our comparative study of wavelet image coders using a perception-based, quantitative picture quality scale as the distortion measure. Coders are evaluated in rate-distortion sense; the influences of different wavelets, quantizers, and encoders are assessed individually. Our results provide an insight into the design issues of optimizing wavelet coders, as well as a good reference for application developers to choose from an increasingly large family of wavelet coders for their applications.

Keywords: wavelets, wavelet transform, image coding and compression, image quality, distortion measure.

1 INTRODUCTION

Research in wavelet image coding since the late 1980's has explored various aspects of wavelet image coders.[1–12] Today, this field continues to grow at a rapid pace; reports on new coders and variations to the existing ones are appearing constantly at conferences and in journals. Despite the widespread interest in wavelet coders, there has been no comprehensive and comparative study of the performance of various wavelet coders using a suitable distortion measure. This makes it difficult to consider optimum designs or to choose from an increasingly large family of wavelet coders for specific applications. We were thus motivated to perform a comparative study of wavelet coders.

Our comparative study is confined to still images and is based on a rate-distortion measure. A common expectation about wavelet image coders is that they produce subjectively better quality images than the standard JPEG coder. This is a well recognized fact, at least for images encoded at low bit-rates. However, an objective evaluation must rely on some quantitative distortion measure. The traditional distortion measure, the mean square error (MSE), has long been recognized as inadequate because of its low correlation with human visual perception. It is particularly inappropriate to use the MSE for evaluating wavelet coders which are largely motivated by the properties of the human visual system (HVS).[13] We chose to use a perception-based, quantitative distortion measure, called the Picture Quality Scale (PQS), in our study. The PQS has been developed in the last few years for evaluating the quality of compressed images. It combines various perceived distortions in image coders into a single quantitative measure; and it correlates well with the subjective evaluation quantified by a mean opinion score (MOS). In previous research, the JPEG image coder, along with one subband and one wavelet coder, was

studied extensively using the PQS.[14]

The design of a wavelet image coder can be divided into three parts: wavelet and related representations, quantization strategies, and error-free encoding techniques. In each part, one has freedom to choose from a pool of candidates and this choice will ultimately affect the coder performance. Therefore, it is necessary to evaluate each choice independently, i.e., with the other parts of the coder fixed. The number of such combinations can be prohibitively large, even after we eliminate some apparently unreasonable choices, so that in this paper, while we review a large number of possible choices for each decision, we present our comparative results using two wavelets, three quantizers, and three encoders on two test images.

The rest of paper is organized as follows: Section 2 reviews the family of wavelet image coders by listing different choices of wavelets, quantizers, and encoders; Section 3 introduces the PQS as a distortion measure; Section 4 presents experimental results of coder comparisons and some comments; Section 5 concludes the paper.

2 FAMILY OF WAVELET IMAGE CODERS

In this section, we review the family of wavelet image coders by examining the options we have for wavelet representations, quantizers, and encoders. Generally speaking, a wavelet image coder can be made by selecting a wavelet representation, a set of quantizers, and an error-free encoder. However, an arbitrary combination of the three parts does not always make sense in practice. We will point this out as we encounter such situations.

2.1 Wavelet Representations

Wavelet representations differ in their choice of wavelets. We shall discuss a few general types of wavelets and the associated representations in the context of image coding. We consider only separable 2-D wavelets which are completely determined by corresponding 1-D wavelets and scaling functions.

Orthogonal Wavelets. These are the family of wavelets that generate orthonormal bases of $\mathbf{L}^2(\mathbf{R}^n)$. Among them the most important ones to image coding are compactly supported orthogonal wavelets. In the discrete wavelet transform (DWT), compactly supported wavelets correspond to FIR filters and thus lead to efficient implementations. A systematic way of constructing compactly supported wavelets was developed by Daubechies,[15] and a fast algorithm for computing a DWT was given by Mallat.[1] Two popular families of compactly supported wavelets are the Daubechies wavelets[15] and Coifman wavelets, or Coiflets.[16] Each family is parameterized by an integer that is proportional to the length of the wavelet filter. For compactly supported wavelets, the length of a wavelet filter is proportional to the degree of smoothness and regularity of the wavelet, which in turn can affect the coding performance. However, studies[2,18] have found that for filter lengths greater than 8 or 10, the gain in compression performance is nominal and not worth the additional computational cost.

A major disadvantage of compactly supported wavelets is their asymmetry. This property translates into nonlinear phase in the associated FIR filters. In computing a DWT using nonlinear phase wavelet filters with finite-length data, a periodic "wrap-around" extension is often used. This may cause artifacts at the borders of the wavelet subbands. These artifacts can be avoided if we use linear phase wavelet filters and a "flip-over" data extension.[1] Symmetry in wavelets and their associated filters can be obtained only if one is willing to give up either compact support or orthogonality of wavelets (except for the Haar wavelet). The use of noncompactly supported wavelets such as the Lemarie-Battle wavelet in image coding has been demonstrated.[1] But, such a choice adds computational burden and is not economical in a hardware implementation of the coder. For example, although the coefficients of the Lemarie-Battle wavelet decay at an exponential rate, we found that 50 coefficients (one side) are needed to achieve a reconstruction accuracy to 6 significant figures. If we want both symmetry and compact support in wavelets, we are led to biorthogonal wavelets.

Biorthogonal Wavelets. The reason for using biorthogonal wavelets is mostly for their symmetry. The price we pay for this is little as far as image coding is concerned. When using biorthogonal wavelets, the quadrature mirror filters (QMF) we use to compute a DWT are no longer an orthogonal pair. They are, however, orthogonal to another QMF pair that we use to compute the inverse DWT. The perfect reconstruction property is preserved, and

Mallat's fast algorithm can still be used. There are also systematic ways of constructing compactly supported biorthogonal wavelets.[19] One can choose, for example, to build filters with similar or dissimilar lengths for decomposition and reconstruction, or which are nearly orthogonal.[5] Since there is little extra cost associated with biorthogonal wavelets, they are adopted in several wavelet image coders.[5,9] However, although the advantages of using linear phase biorthogonal filters in image coding have been conjectured,[17] a previous study by Rioul[18] did not clearly indicate this.

Wavelet Packets. Coifman *et al.*[20] introduced wavelet packets as a generalized family of multiresolution orthogonal or biorthogonal bases that includes wavelets. A family of wavelet packet bases can be generated by the same QMF pair that generate the wavelet. An extensive coverage on this topic can be found in a book by Wickerhauser.[21] From subband coding point of view, any subtree sharing the same root with the full subband tree corresponds to an orthogonal or biorthogonal representation using a specific member of the wavelet packet bases generated by a QMF pair. Clearly, one can choose from this rich family a "best" basis by some criterion. Coifman and Wickerhauser[4] developed entropy-based algorithms for best basis selection. Their algorithm converges to a minimum-entropy basis. Note that the "entropy" in Coifman and Wickerhauser's algorithm is a measure of energy compaction of a vector. Since natural images usually have their energy concentrated in low frequency bands, one would imagine that an entropy-based algorithm would converge to the wavelet basis, which is often indeed the case. Another algorithm for determining the best basis in a rate-distortion sense was developed by Ramchandran and Vetterli.[10] If one is concerned primarily with lossy compression, the best basis that minimizes the total distortion for a given bit-rate is clearly preferable to a minimum-entropy basis.

Zero-Crossings and Local Maxima of Wavelet Transforms. Under certain conditions, an image can be effectively represented by the zero-crossings of the wavelet transform[22] or local maxima of the wavelet transform modulus.[12] When wavelets are carefully chosen as a smoothed gradient operator, the zero-crossings and local maxima of corresponding wavelet transforms can be interpreted as "multiscale edges". Generally speaking, a non-orthogonal wavelet is required for this purpose and the resulting wavelet transform of the image is oversampled in space before the extraction of the zero-crossings and local maxima. Image coding using zero-crossings and local maxima was demonstrated by Mallat[22] and Mallat and Zhong.[23] The latter was refined by Froment and Mallat[24] and linked to the "second-generation image coding techniques"[25] that use image features such as contours, as coding primitives. A more recent coding system along this line was developed by Croft and Robinson.[26] These feature-based image coding systems usually require non-conventional quantization and encoding techniques. For example, in the wavelet local maxima representation, coding performance would be better if quantization is done on the chains of local maxima (edge contours) instead of individual local maxima.[12] The quantized chains of wavelet local maxima can then be encoded with a contour coder.[27]

2.2 Quantization Techniques

Scalar Quantization (SQ). Suppose we have decomposed an image to N dyadic scales using a wavelet transform or wavelet packet transform, either orthogonal or biorthogonal. This will yield $3N + 1$ wavelet subbands. Since the variance of each subband is generally different, we need to design a quantizer for each subband. If we assume the encoder employed at the later stage uses variable-length codewords, we are led to consider only uniform quantizers.[28] In this case the design of a uniform scalar quantizer boils down to the choice of a quantizer step-size for each subband. A simple but rather arbitrary design could be to start with some step-size q_0, and decrease it by a factor of 2 for all three oriented subbands as one goes to the next coarser scale. The lowest subband is often finely quantized using the smallest possible step-size. The q_0 can be determined by matching the averaged entropy of all quantized subbands to the given total bit-rate. This design is obviously nonoptimal, but works satisfactorily in practice as evidenced by the EPIC software.[29] More sophisticated quantizer designs can take into account the characteristics of the HVS, or an optimally allocated bit budget for each subband. Lewis and Knowles[7] designed a HVS-weighted quantizer that takes into account the HVS' spectral response, noise sensitivity in background luminance, and texture masking. If the bit budget has been allocated for each subband, then an entropy-constrained optimum quantizer can be designed.[30] The problem of optimal bit allocation in the context of wavelet image coding was addressed in several papers.[5,31,33]

Vector Quantization (VQ). Vector quantization is a generalization of scalar quantization in which vectors, or blocks, of pixels are quantized instead of the pixels themselves. The general optimality of VQ over SQ was discussed by Gersho and Gray.[32] To apply VQ to wavelet image coding, the common approach is still to consider each subband individually. In the work of Antonini *et al.*,[5] a subcodebook is generated for each subband, and a multiresolution codebook is obtained by assembling all subcodebooks. Senoo and Girod[33] compared several VQ algorithms for subband image coding and concluded that entropy-constrained VQ gives the best performance, and that lattice VQ performs is only slightly worse, but with a much simpler implementation. Since subbands are a hierarchical organization of oriented frequency bands, it is intuitive to consider quantizing a vector whose elements span subbands of the same orientation. This idea, however, does not lead to a new form of VQ; it leads to a new quantization strategy, referred to as "space quantization".

Space vs. Frequency Quantization. We refer to the technique of designing quantizers, either scalar or vector, for each individual subband as "frequency quantization" since each subband corresponds a different frequency range. Since wavelet representations have both scale (frequency) and space contents, spatial grouping of data and quantization are possible. However, this is somewhat beyond the scope of conventional quantizer design because the number of samples corresponding to the same location in the same orientation is decreased by a factor of 4 as we move from fine to coarse scale subbands. Shapiro[11] designed an elegant method, called the *embedded zerotree wavelet algorithm (EZW)*, to turn this difficulty into an advantage. Quantization is done by successive approximation across the subbands with the same orientation. This results in an efficient data structure for encoding zero and nonzero quantized values. More recently, studies on joint space-frequency quantization[34,35] attempt to fully exploit the space-frequency characteristics of wavelet representations.

2.3 Error-Free Encoding Techniques

Huffman Code and Run-Length Encoding. Although not an actual encoding technique, band based Shannon entropy is commonly used in the evaluation of coding performance. A simple encoding technique results if Huffman codes are designed for each band. Care must be exercised, however, to insure that accurate statistics are used to design these codes. One can design a universal code based on an ensemble of typical images or explicitly transmit the Huffman codes, along with the compressed image data, to the decoder. For highly skewed sources, such as quantized wavelet transformed images, Huffman codes are known to be very inefficient. But, if the most probable symbols (zeros) are removed from the source and encoded separately, little spatial correlation remains among the non-zero values, which can then be encoded efficiently. Commonly, run-length encoding the abundance of zeros, when combined with Huffman encoding of the non-zero values, produces good results.[6,9]

Arithmetic Code. Adaptive arithmetic codes start with no information about the image and implicitly transmit the model to the decoder in the compressed data stream, therefore, are free from the ensemble issues associated with the design of Huffman codes. Binary arithmetic codes, such as the Q-code and QM-code,[37] are more computationally efficient than their multi-alphabet counterparts,[36] but require a mapping from the quantized coefficients to a sequence of binary decisions. A simple technique, which is similar to the run-length encoding discussed above, proves to be very beneficial. The locations of the non-zero pixels are specified by encoding a binary *activity mask* (all non-zero values are set to 1) with standard binary image compression techniques, such as JBIG, after which the non-zero pixels are mapped through a balanced binary tree and encoded. Using such a technique, we often obtain bit-rates less than the Shannon entropy (based on independent pixels) due to the significant spatial correlation between the zeros in a wavelet transformed image. An alternative, efficient representation of the zeros in the source is exploited by Shapiro's zerotree[11] coder.

3 PICTURE QUALITY SCALE (PQS)

Research into the psychophysics of human visual perception has revealed that the HVS is not equally sensitive to various types of distortion in an image. This directly affects the perceived image quality. The PQS is based on quantitative measures of several distortion factors. Because these distortion factors are correlated, a principal

component analysis is done to transform them into uncorrelated "sources of errors", and dominant sources are identified. These errors are then mapped to a PQS value by a model which was obtained from a linear regression analysis with the Mean Opinion Score (MOS).

3.1 Distortion Factors

The current version of the PQS includes five distortion factors of which the first two are derived from random errors and the last three from structural errors. Here we give only a description of these distortion factors. Formulas for computing the actual numerical measures are detailed in two references.[14,38]

Distortion Factor F_1 is a weighted difference between the original and the compressed images. The weighting function adopted is the CCIR television noise weighting standard. Here the viewing distance is assumed to be four times the picture height.

Distortion Factor F_2 is also a weighted difference between the original and the compressed images. The weighting function is from a model of the HVS. In addition, an indicator function is included to account for the perceptual threshold of visibility.

Distortion Factor F_3 reflects the end-of-block disturbances. The HVS is quite sensitive to linear features in images. In block coders, the error image contains discontinuities at the end of blocks, which explains blocking artifacts in the compressed image.

Distortion Factor F_4 accounts for general correlated errors. Textures with strong correlation are more perceptible than random patterns. The error image having strong correlation suggests more apparent distortion in the image to human viewers.

Distortion Factor F_5 is a measure of the large errors that occur for most coders in the vicinity of high contrast transitions (edges). Two psychophysical effects occur in the vicinity of high contrast edges. On the one hand, the visibility of noise decreases; this is referred to as "visual masking". On the other hand, the visibility of misalignments increases.

3.2 Principal Component Representation of Distortion Measures

Because the distortion factors $\{F_i\}_{1\leq i\leq 5}$ are correlated, a principal component analysis is performed to decorrelate distortion measures and identify the dominant sources. This is done for a test set of distorted images obtained from representative coders. Table 1 lists a covariance matrix of $\{F_i\}$, C_F, which was computed from a set of 24 distorted images obtained by encoding two reference images with transform and DPCM coders for a range of quality scales. An eigen analysis on C_F gave the transform matrix that decorrelates $\{F_i\}$. It was found out that among the five eigenvalues of C_F the three largest ones accounts for 98% of the total error energy. Therefore, the three eigenvectors corresponding to the three largest eigenvalues can be chosen to transform $\{F_i\}$ into a principal component representation, $\{Z_i\}_{1\leq i\leq 3}$.

3.3 Formation of the PQS

Since the various distortion factors collectively contribute to the overall perceived image quality, we seek a functional model mapping the distortion factors or measures to a single quality scale, the PQS. This model can be experimentally determined by studying the functional relationship between the distortion measures and the MOS, a five scale subjective ranking of image quality in terms of perceived distortions that are described in Table 2.[39] The simplest model is a linear one in which the PQS is expressed as a linear combination of uncorrelated principal distortion measures, $\{Z_i\}$, that is,

$$PQS = b_0 + \sum_{i=1}^{3} b_i Z_i$$

Table 1: Covariance Matrix of F_i

	F_1	F_2	F_3	F_4	F_5
F_1	1.00	0.97	0.95	0.03	0.97
F_2	0.97	1.00	0.99	0.15	0.91
F_3	0.95	0.99	1.00	0.17	0.88
F_4	0.03	0.15	0.17	1.00	0.11
F_5	0.97	0.91	0.88	0.11	1.00

Table 2: The Scales of the MOS

Grading Scales	Impairment
5	Imperceptible
4	Perceptible, but not annoying
3	Slightly annoying
2	Annoying
1	Very Annoying

where $\{b_i\}_{0 \le i \le 3}$ are the partial regression coefficients obtained by multiple linear regression of $\{Z_i\}$ against the MOS.[38,40] Nonlinear models have also been studied that employ neural networks to compute the PQS.[41,42]

For the aforementioned set of 24 distorted images, the MOS values were obtained from an experiment involving nine observers under the conditions specified by the CCIR.[39] The observers were allowed to give half scale scores. A multiple linear regression analysis of $\{Z_i\}$ against the MOS gave $b_0 = 6.431$, $b_1 = -0.069$, $b_2 = -1.475$, $b_3 = -0.136$, with correlation coefficient $R = 0.88$.

4 RESULTS AND COMMENTS

In this section we present some results from our comparative study of several wavelet coders. The comparison is in the rate-distortion sense where the distortion is measured by the PQS. Two popular test images, Lenna and Barbara, both 256×256, were used in the experiment. A total of 266 encoded images were compared, representing a combination of two wavelets, three quantizers, and three encoders, plus the EZW coder for coding the two test images at seven bit-rates ranging from 0.5 to 2.0 bpp. The two wavelets used are the orthogonal, 8-tap wavelet of Daubechies (D8)[15] and the biorthogonal, "9-7" wavelet of Barlaud (B97).[5,17] All wavelet transforms are computed for 4 dyadic scales, resulting in 13 subbands. All three quantizers are scalar quantizers: the first is the non-optimized quantizer (Q1) described in Section 2.2; the second is the HVS-weighted quantizer (Q2) of Lewis and Knowles[7]; the third is an entropy-constrained quantizer (Q3) where a bit budget is optimally allocated to each subband and used as a constraint in the quantizer design.[30,31] All three encoders are band based, i.e., each band is processed separately. They are: a simple Huffman encoder (E1), run-length encoded zeros plus Huffman encoded non-zero values (E2), and the activity mask based technique discussed in Section 2.3, where we QM-encode the mask using a 7-pixel spatial predictive context and the non-zero values using binary tree decomposition (E3). In addition, we tested the EZW coder with the B97 wavelet, tree-structured spatial quantization, and adaptive arithmetic encoding.

The results are organized and presented in several ways. In assessing the choice of wavelets and quantizers, we use the computed entropy H of a quantized wavelet representation as the bit-rate, assuming we have an ideal entropy encoder. The two wavelets {B97,D8} are compared for fixed quantizers and the three quantizers {Q1,Q2,Q3} are compared for fixed wavelets. To compare the three encoders, we plot actual bit-rate outputs from {E1,E2,E3} versus H (which is the lower bound on bit-rate if pixels are independent). Finally, we compare the overall performance of a few coders synthesized from different choices of wavelets, quantizers, and encoders.

4.1 Comparison of Two Wavelets

Figure 1 contains six plots comparing B97 with D8 for fixed quantizers, {Q1,Q2,Q3}. In all cases B97 leads D8, by as much as 0.43 PQS for a given bit-rate or 0.2 bpp for a given PQS value. Note that filters of B97 and D8 have similar lengths. The advantage of biorthogonal wavelets over orthogonal wavelets is clear and consistent in this experiment.

4.2 Comparison of Three Quantizers

Figure 2 compares our three quantizers for fixed wavelets, {B97,D8}. We find that Q2 is the winner in most cases. For low bit-rates, Q2 is sometimes slightly outmatched by one of the other quantizers. At higher rates, Q2's dominance increases. Recall that Q2 is a HVS-weighted quantizer. Its advantage is not obvious when we examined the peak signal-to-noise ratios (PSNR). In fact, the difference between the three quantizers by PSNR is within 0.2 dB for all bit-rates tested. This shows that PQS indeed takes into account the characteristics of the HVS. No clean relationship between Q1 and Q3 can be derived from our results; Q3 beats Q1 for Lenna, but the situation is reversed for Barbara, though by different degree.

4.3 Comparison of Three Encoders

Figure 3 shows the output bit-rates of three encoders versus computed entropies for Lenna and Barbara. Similar results were observed for all wavelets and quantizers, therefore, to reduce the number of plots presented, we averaged the results across wavelets and quantizers to produce the composite results shown. In each plot we also draw a line of unit slope where the output bit-rate equals the entropy. As expected, the simple Huffman encoder (E1) always gives a bit-rate higher than the entropy, especially at low bit-rates where there are a large number of zeros, i.e., when the source is highly skewed. When combined with run-length encoding of the zeros (E2), the results are much better, and only slightly worse than our best, activity mask based technique. We must point out, though, that our Huffman code results are image specific and do not include the overhead of transmitting 13 (one per subband) Huffman codes to the decoder. Therefore, the bit-rates for E1 and E2 in Figure 3 are lower bounds on the rate of a more realistic such code. We did not compute the cost of transmitting the Huffman codes or consider the design of a generic Huffman code based on an appropriate ensemble of images because the results for code E3 are better and do not ignore any hidden costs. We observe that E3's bit-rates are consistently lower than the (independent pixel) entropy, which may appear counterintuitive to some, but is correct since we are exploiting spatial dependencies in the source which are not reflected in the entropy computation. Note that by using E3 we can obtain bit-rates as much as 0.3 bpp below the entropy. We declare E3 the winner.

4.4 Comparison of Wavelet Coders

We now compare a few complete wavelet image coders synthesized from different wavelets, quantizers, and encoders. A combination of "the best" gives the B97-Q2-E3 for both Lenna and Barbara. We also present D8-Q1-E3 and D8-Q1-E1 for Lenna and D8-Q3-E3 and D8-Q3-E1 for Barbara. These coders along with the EZW coder are compared in Figure 4. For Barbara, B97-Q2-E3 is the sure winner followed by the EZW and D8-Q3-E3. For Lenna, B97-Q2-E3 is the winner for most bit-rates, with EZW winning at high bit-rates. For both images, the simple Huffman encoder yields, clearly, the poorest coder. Of course, an intelligent designer would not choose such a code. Our results only indicate how bad such a brute force design can be.

The EZW coder is, in our mind, the state-of-the-art in wavelet image coding. The fact that we can make an even better coder (in terms of PQS vs. bit-rate) just by assembling available techniques testifies to the value of good synthesis in wavelet coder design. Comparing the EZW with B97-Q2-E3, we found that both exploit dependency between quantized coefficients for encoding, which provides the possibility to achieve bit-rates below the entropy. The difference is that B97-Q2-E3 exploits intraband dependency by encoding the activity masks while the EZW exploits interband dependency by encoding the zerotrees. While the zerotrees take advantage of the space-scale characteristics of wavelet representations, we noticed that the EZW's performance becomes relatively poor at low bit-rates, suggesting its higher overhead for encoding the zerotrees. For quantization, the EZW uses successive approximation, while B97-Q2-E3 uses a HVS-weighted quantizer which contributes to its higher performance as measured by the PQS. Lastly, the good performance of D8-Q3-E3 and D8-Q1-E3 suggests that the effect of different wavelets (of similar filter lengths) is less significant than that of quantizers and encoders.

5 CONCLUSION

We have presented some results from a comparative study of different wavelet image coders using a perception-based picture quality scale. While these results provide a good reference for application developers to choose a good wavelet coder for their applications, they also shed some light on issues of optimum design of wavelet coders. Our work shows that an excellent wavelet coder can result from a careful synthesis of existing techniques of wavelet representation, quantization, and error-free encoding. Exploiting the dependency of quantized coefficients, including zeros, is a very effective way to boost the overall performance of a wavelet coder. Quantizers designed with considerations of the characteristics of HVS also show advantages when an appropriate distortion measure is used. The effect of variations between asymmetric orthogonal and symmetric biorthogonal wavelets is also noticeable, but less significant when compared with the other two factors.

6 ACKNOWLEDGMENT

We would like to thank A. Kris Huber of Utah State University for providing us with his implementation of the EZW coder. We also acknowledge support of the UC Micro Program, Hewlett-Packard, Lockheed, and Pacific Bell.

7 REFERENCES

[1] S.G. Mallat, "A theory of multiresolution signal decomposition: the wavelet representation," *IEEE Trans. Pattern Anal. and Machine Intell.*, vol. PAMI-11, pp. 674-693, July 1989.

[2] W.R. Zettler, J. Huffman, and D.C.P. Linden, "Application of compactly supported wavelets to image compression," *Proceedings of SPIE, Image Processing Algorithms and Applications*, Vol. 1244, pp. 150-160, 1990.

[3] R.A. DeVore, B. Jawerth, and B.J. Lucier, "Image compression through wavelet transform coding," *IEEE Trans. on Information Theory*, Vol. 38, pp. 719-746, Mar. 1992.

[4] R.R. Coifman and M.V. Wickerhauser, "Entropy-based algorithms for best basis selection," *IEEE Trans. Infor. Theory*, Vol. 38, pp. 713-718, Mar. 1992.

[5] M. Antonini, M. Barlaud, P. Mathieu, and I Daubechies, "Image coding using wavelet transform," *IEEE Trans. on Image Processing*, Vol. 1, pp. 205-220, Apr. 1992.

[6] J.N. Bradley, C.M Brislawn, and T. Hopper, "The FBI wavelet/scalar quantization standard for grayscale fingerprint image compression," *Proc. of SPIE, Visual Info. Proc. II*, Orlando, FL, Apr. 1992, pp. 293-304.

[7] A.S. Lewis and G. Knowles, "Image compression using the 2-D wavelet transform," *IEEE Trans. on Image Processing*, Vol. 1, pp. 244-250, Apr. 1992.

[8] M. Ohta, M, Yano, and T. Nishitani, "Wavelet picture coding with transform coding approach," *IEICE Trans. Fundamentals*, Vol. E75-A, pp. 776-785, July 1992.

[9] C.K. Cheong, K. Aizawa, T. Saito, and M. Hatori, "Subband image coding with biorthogonal wavelets," *IEICE Trans. Fundamentals*, Vol. E75-A, pp. 871-881, July 1992.

[10] K. Ramchandran and M. Vetterli, "Best wavelet packet bases in a rate-distortion sense," *IEEE Trans. Image Processing*, Vol. 2, pp. 160-175, Apr. 1993.

[11] J.M. Shapiro, "Embedded image coding using zerotrees of wavelet coefficients," *IEEE Trans. on Signal Proc.*, Vol. 41, pp. 3445-3462, Dec. 1993.

[12] S.G. Mallat and S. Zhong, "Characterization of signals from multiscale edges," *IEEE Trans. Pattern Anal. and Machine Intell.*, vol. PAMI-14, pp. 710-732, July 1992.

[13] S.G. Mallat, "Multifrequency channel decomposition of images and wavelet models," *IEEE Trans. Acoust. Speech and Signal Proc.*, Vol. 37, pp. 2091-2110, Dec. 1989.

[14] V.R. Algazi, Y. Kato, M. Miyahara, and K. Kotani, "Comparison of image coding techniques with a Picture Quality Scale," *Proceedings of SPIE, Applications of Digital Image Processing XV*, Vol. 1771, 1992.

[15] I. Daubechies, "Orthonormal bases of compactly supported wavelets," *Comm. Pure Appl. Math.*, Vol. 41, pp. 909-996, 1988.

[16] I. Daubechies, "Orthonormal bases of compactly supported wavelets II, Variations on a theme," *SIAM J. Math. Anal.*, Vol. 24, pp. 499-519, Mar. 1993.

[17] I. Daubechies, *Ten Lectures on Wavelets*, SIAM, Philadelphia, PA, 1992.

[18] O. Rioul, "On the choice of 'wavelet' filters for still image compression," *Proceedings of ICASSP'93*, Vol. V, pp. 550-553.

[19] A. Cohen, I. Daubechies, and J.-C. Feauveau, "Biorthogonal bases of compactly supported wavelets," *Comm. Pure Appl. Math.*, Vol. 45, pp. 485-500, 1992.

[20] R.R. Coifman, Y. Meyer, S.R. Quake, and M.V. Wickerhauser, "Signal processing and compression with wavelet packets," in *Proc. of Intl. Conf. on Wavelet Applications*, Toulouse, France, 8-13 June 1992, pp.77-93.

[21] M.V. Wickerhauser, *Adapted Wavelet Analysis from Theory to Software*, A K Peters, Wellesley, MA, 1994.

[22] S.G. Mallat, "Zero-crossings of a wavelet transform," *IEEE Trans. Inform. Theory*, vol. IT-37, pp. 1019-1033, July 1991.

[23] S.G. Mallat and S. Zhong, "Compact image coding from multiscale edges," in *Proc. Intl. Conf. Acoust. Speech and Signal Proc.*, Toronto, May 1991.

[24] J. Froment and S. Mallat, "Second generation compact image coding with wavelets," in *Wavelet: A Tutorial in Theory and Applications,* C.K. Chui, Ed., Academic Press, San Diego, 1992.

[25] M. Kunt, A. Ikonomopoulos and M. Kocher, "Second-generation image-coding techniques," *Proc. of IEEE*, Vol. 73, pp. 549-574, April, 1985.

[26] L.H. Croft and J.A. Robinson, "Subband image coding using watershed and watercourse lines of the wavelet transform," *IEEE Trans. Image Proc.*, Vol. 3, pp. 759-772, Nov. 1994.

[27] S. Carlsson, "Sketch based coding of grey level images," *Signal Processing*, Vol. 15, pp. 57-83, 1988.

[28] A.K. Jain, *Fundamentals of Digital Image Processing*, Prentice-Hall, Englewood Cliffs, NJ, 1989.

[29] E.P. Simoncelli and E.H. Adelson, "Efficient Pyramid Image Coder (EPIC)," a public domain software available from URL: ftp://whitechapel.media.mit.edu/pub/epic/epic.tar.Z

[30] R.C. Wood, "On optimum quantization," *IEEE Trans. Infor. Theory,* Vol. IT-15, pp. 248-252, Mar. 1969.

[31] J. Chen, S. Itoh, and T. Hashimoto, "Scalar quantization noise analysis and optimal bit allocation for wavelet pyramid image coding," *IEICE Trans, Fundamentals,* Vol. E76-A, pp. 1502-1514, Sep. 1993.

[32] A. Gersho and R.M. gray, *Vector Quantization and Signal Compression*, Kluwer Academic Publishers, Boston, 1992.

[33] T. Senoo and B. Girod, "Vector quantization for entropy coding of image subbands," *IEEE Trans. Image Proc.*, Vol. 1, pp. 526-533, Oct. 1992.

[34] Z. Xiong, K. Ramchandran, and M.T. Orchard, "Joint optimization of scalar and tree-structured quantization of wavelet image decompositions," *Proc. 27th Annual Asilomar Conf. on Signal, Syst. and Computers*, Pacific Grove, CA, Nov. 1993, pp. 891-895.

[35] Z. Xiong, K. Ramchandran, M.T. Orchard, and K. Asai, "Wavelet packets-based image coding using joint space-frequency quantization," *Proc. IEEE Intl. Conf. Image Proc.*, Austin, TX, Nov. 1994, Vol. III, pp. 324-328.

[36] I.H. Witten, R.M. Neal, and J.G. Cleary, "Arithmetic coding for data compression," *Comm. ACM*, Vol. 30, pp. 520-539, jun. 1987.

[37] W.B. Pennebaker, J.L. Mitchell, G.G. Landon, Jr., and R.B. Arps, "An overview of the basic principles of the Q-coder adaptive binary arithmetic coder," *IBM J. Research and Development*, Vol. 32 pp. 717-726, Nov. 1988.

[38] M. Miyahara, K. Kotani, and V.R. Algazi, "Objective Picture Quality Scale (PQS) for image coding," *Proc. SID Symposium for Image Display*, 44.3: pp. 859-862, May 1992.

[39] CCIR, "Rec. 500-2, Method for the subjective assessment of the quality of the television pictures," Vol. 11, pp. 165-168, 1982.

[40] M. Miyahara, K. Kotani, Y. Horita, and T. Fujimoto, "Objective Picture Quality Scale (PQS)—Consideration of local feature and universality," *IEICE Trans. B-I,* Vol. J73-B-I, pp. 208-218, Mar. 1990. (in Japanese).

[41] K. Kotani and M. Miyahara, "Objective picture quality scale by neural network (PQS-NN)," *IEICE Trans. B-I*, Vol. J73-B-I, pp. 347-352, Apr. 1990. (in Japanese).

[42] K. Kotani and M. Miyahara, "Objective picture quality scale by neural network fed the distortion factors to the input layers," *IEICE Trans. D-II*, Vol. J73-D-II, pp. 1303-1308, Aug. 1990. (in Japanese).

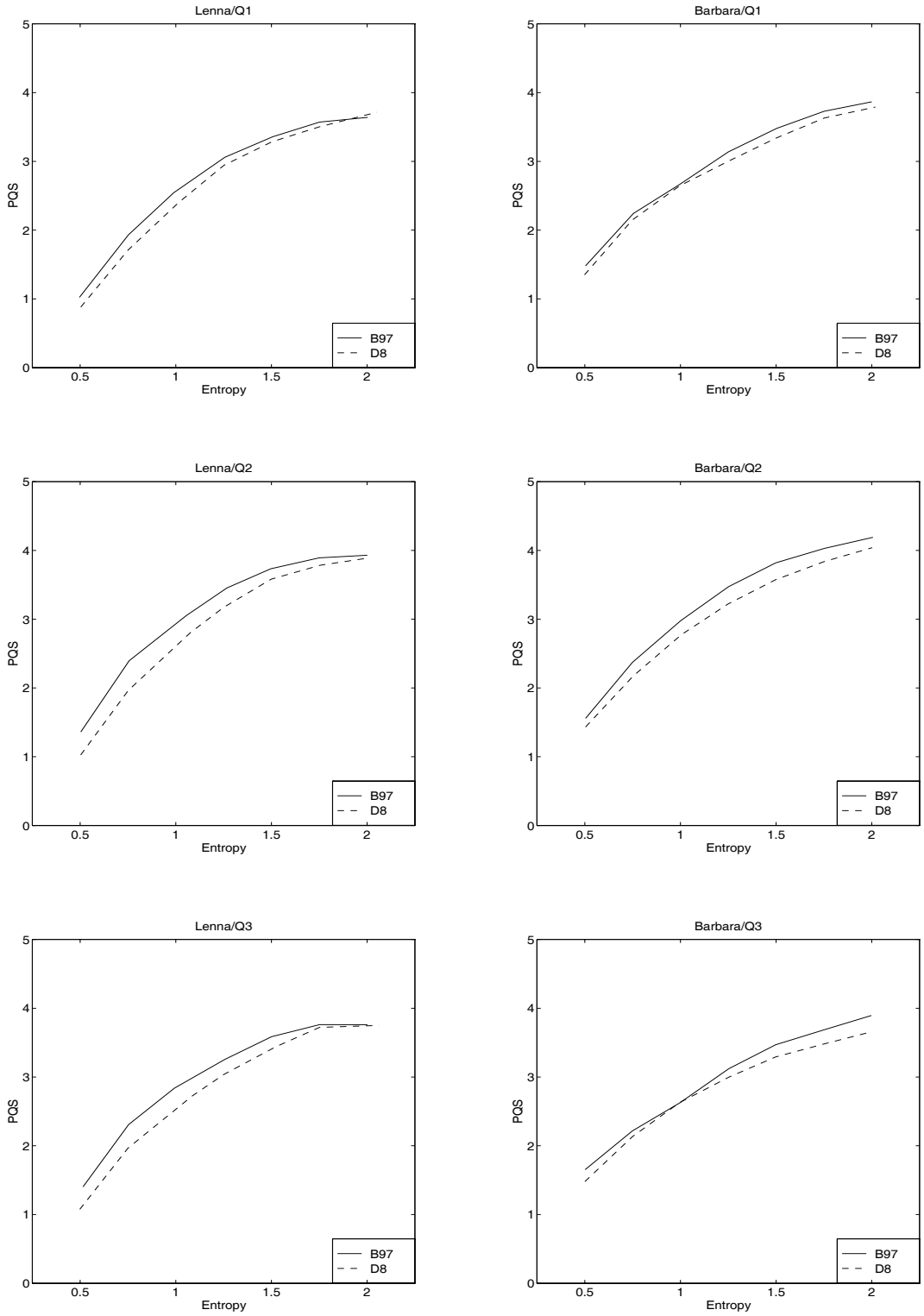

Figure 1: Comparison of two wavelets, {W97,D8}. Left and right columns are for Lenna and Barbara, respectively. *Top:* comparison under quantizer Q1; *Middle:* comparison under quantizer Q2; *Bottom:* comparison under quantizer Q3.

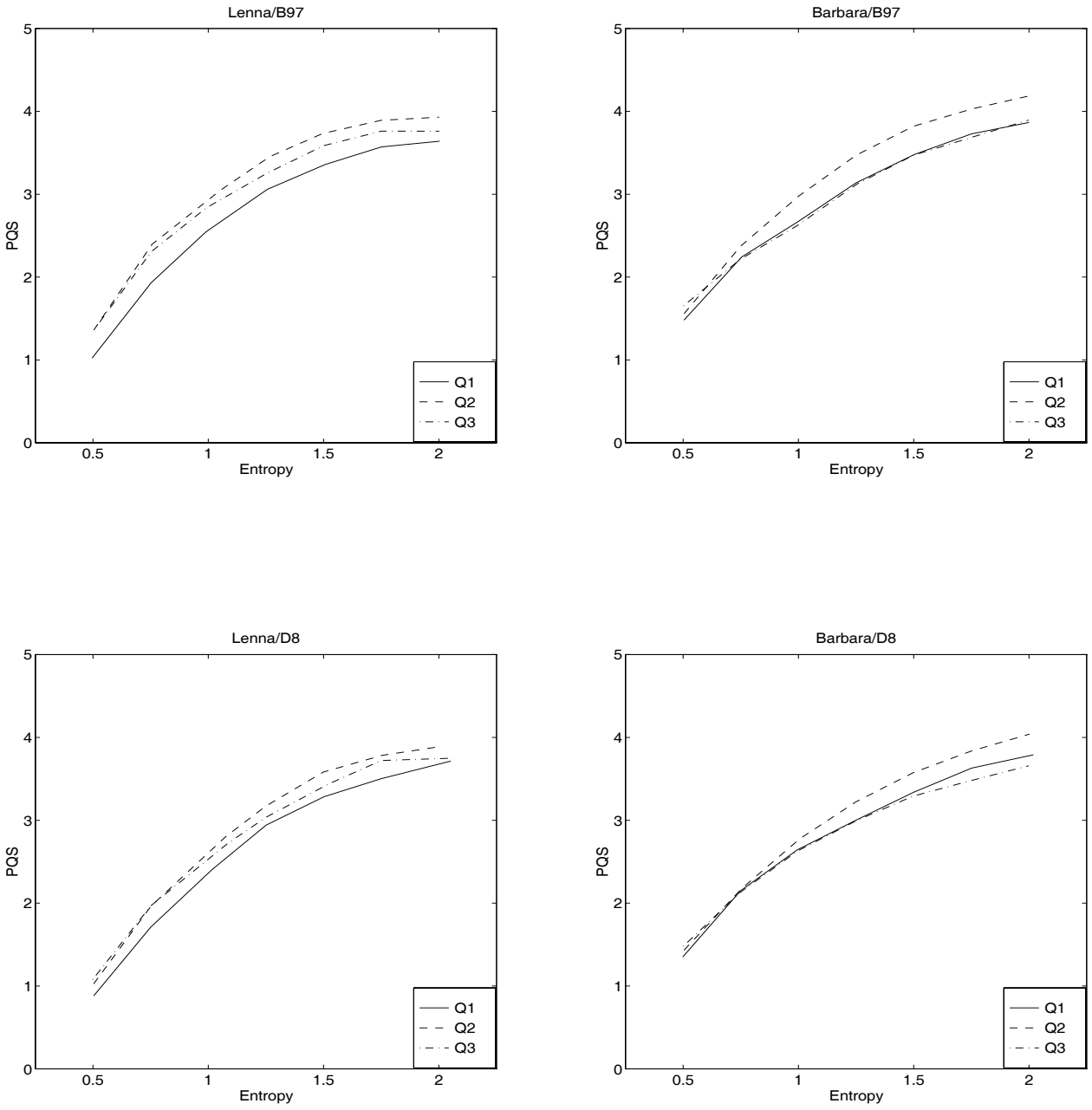

Figure 2: Comparison of three quantizers, {Q1,Q2,Q3}. Left and right columns are for Lenna and Barbara, respectively. *Top:* comparison under wavelet B97; *Bottom:* comparison under wavelet D8.

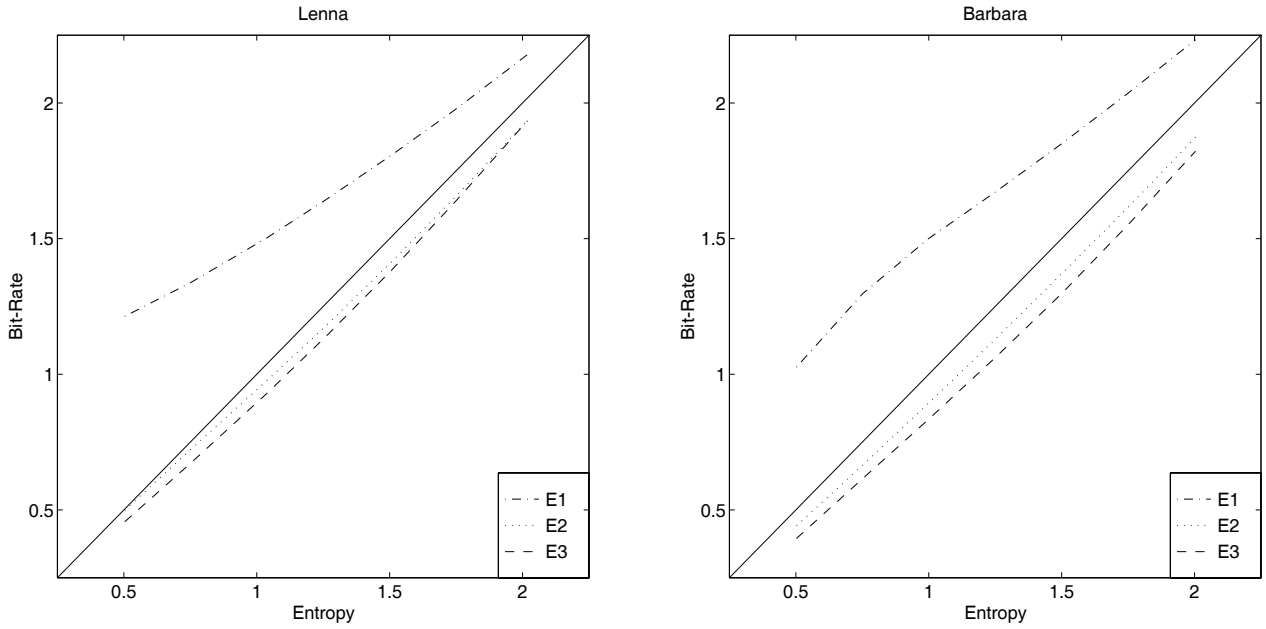

Figure 3: Comparison of three encoders, {E1,E2,E3}. Bit-rates are averaged over {B97,D8} and {Q1,Q2,Q3} for the same images. *Left:* comparison for Lenna; *Right:* comparison for Barbara.

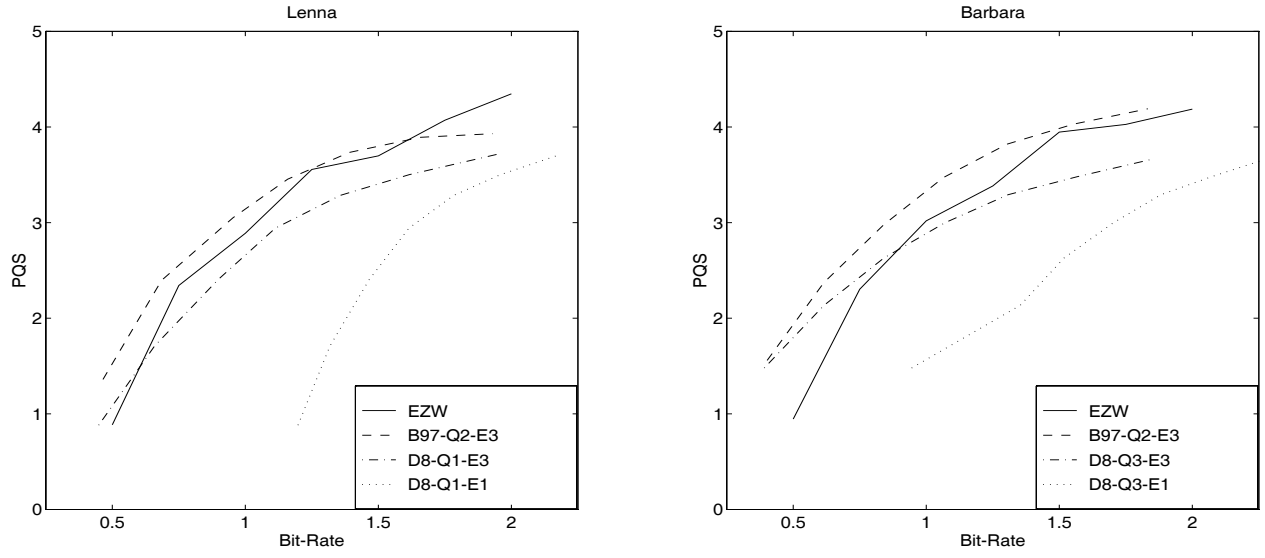

Figure 4: Comparison of four wavelet image coders. *Left:* comparison for Lenna; *Right:* comparison for Barbara.